

SUPPLEMENTAL MATERIAL

SUPPLEMENTAL METHODS

Murine studies

Endothelium-specific CNP^{-/-} were developed in house¹, global NPR-B^{-/-} (Peewee)² were the kind gift of Prof. S. Camper (University of Michigan), and global NPR-C^{-/-3} were the kind gift of Prof. O. Smithies (University of North Carolina). Mice were housed in a climatically controlled environment, on a 12 h light/dark cycle, with free access to water and standard food *ad libitum*.

Clinical samples

All patients involved in the study were provided with written and verbal information prior to consenting. Patients undergoing above or below knee amputation for CLI secondary to PAD at the Royal Free Hospital were identified and consented. Immediately after limb amputation, the deep belly of the gastrocnemius muscle was identified on the amputated remnant and a 1 cm³ biopsy excised. Control samples were taken from consented patients undergoing coronary artery bypass graft without PAD (ankle-branchial index = 1.0 to 1.4) at St Bartholomew's Hospital. During open saphenous vein harvesting, the deep belly of the gastrocnemius was identified and a 0.5cm³ muscle biopsy was excised. Upon collection, tissue was immediately divided in to two portions for further analysis. One portion was fixed in 10% formal saline containing 4% formaldehyde (CellStor Pot, CellPath Ltd, UK) prior to dehydrating for subsequent embedding and immunohistochemical analysis. A second portion was collected and treated with an RNA stabilizer (RNAlater, Sigma, UK) and stored at -20°C before RNA isolation.

Natriuretic peptide receptor expression & immunoblotting

RNA was extracted from cells and tissues using a mini RNA extraction kit (Qiagen, UK) and quantified using a NanoDrop spectrophotometer (Thermo Scientific, MA, USA). RNA was subsequently converted to cDNA by reverse transcription (Quantitect Reverse Transcription kit, Qiagen, UK). For cells, 20 ng of cDNA from each sample was added to NPR-C and NPR-B Taqman gene expression assays and was amplified using quantitative real-time PCR over 40 cycles. For both human and mouse tissue samples, 10ng of cDNA from each sample was used for qPCR using a SYBR-green based PCR mix (SensiFast SYBR NO ROX; Bioline, UK) and primers from the specific gene of interest, followed by PCR in the thermal cycler (CFX Connect Realtime System, Biorad, UK) over 39 cycles. Samples were subjected to melting curve analysis to confirm amplification specificity. mRNA expression was analyzed by expressing the cycle threshold (Ct) value as $2^{-\Delta\Delta C_t}$, relative to the levels of *RPL19* for tissue samples and *GAPDH* for cells, and further normalized as a fold change to control treatments. Primer sequences are provided in **Supplemental Table 1**.

Standard sodium dodecyl sulfate polyacrylamide gel electrophoresis (SDS-PAGE) protocols were employed to identify protein expression using the following antibodies: NPR-C (1:500; Abcam), p42/44 MAPK (ERK1/2, 1:1000, 4696S), phosphor-p42/44 MAPK (p-ERK1/2, 1:1000, 9101S), Akt (1:1000), phosphor-Akt (1:1000; all Cell Signaling Technology, MA, USA). GAPDH (1:4000, AM4300; ThermoFisher Scientific, Hemel Hempstead, UK) or β -actin (1:5000; Millipore, UK) was used as loading control.

Histological and immunofluorescence analysis

Gastrocnemius muscles were harvested from ischemic and non-ischemic limbs of all animals at 28 days following HLI, and from control and HLI patients fixed in 4% paraformaldehyde (overnight, 4°C). Following routine paraffin wax embedding, transverse sections (6 µm) were prepared using a microtome onto poly-L-lysine slides. Sections were allowed to dry overnight and stained with H&E for histological analysis. The proportion of fibers with central nuclei (regenerating fibers) was counted in the cross-sectional areas from both the injured and non-injured areas of both limbs, in a blinded fashion.

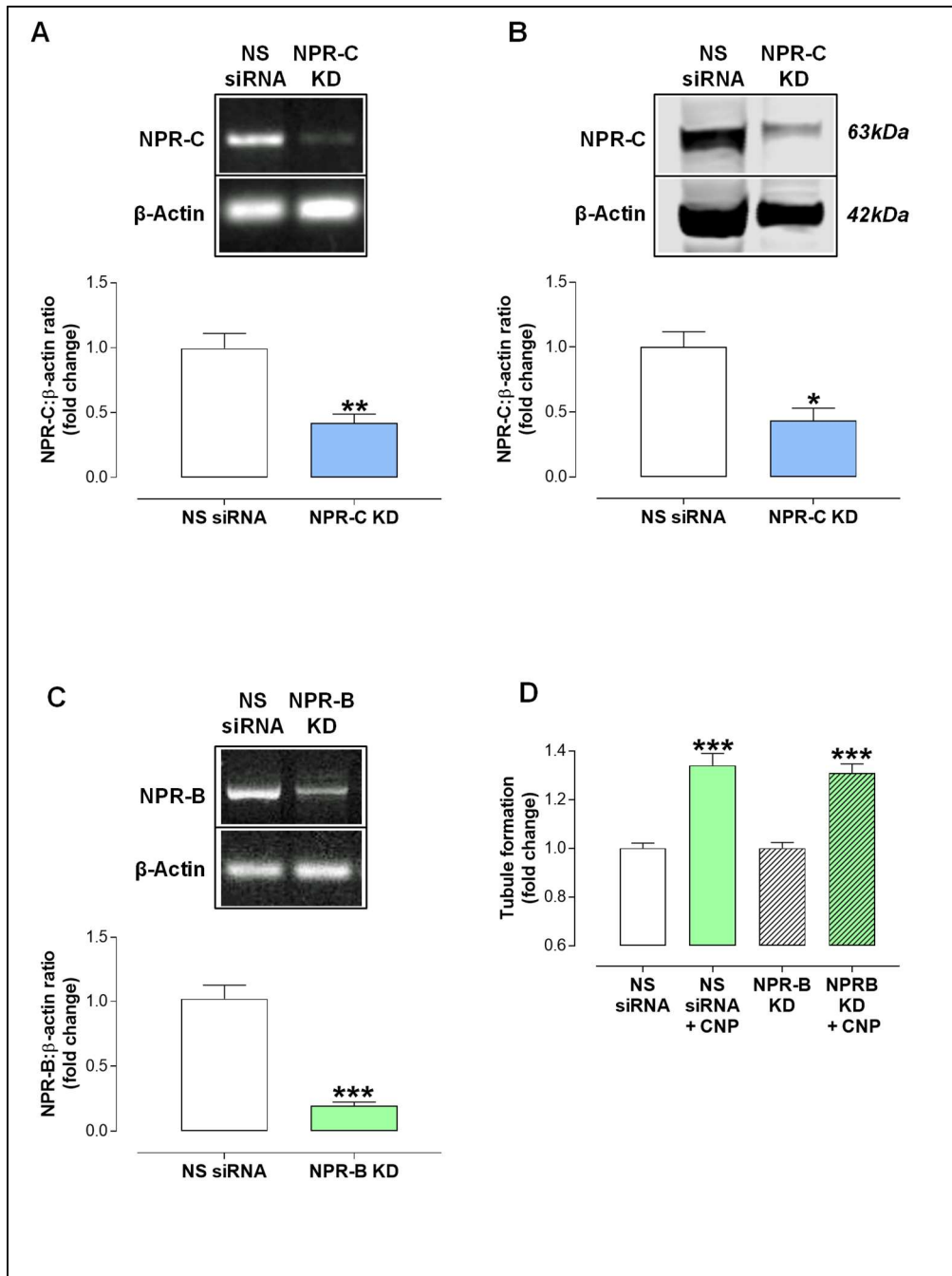
Picrosirius red (0.1 % w/v) staining was used to visualize collagen fibers in the muscle and fibrosis was assessed blindly (Picrosirius Red Stain kit; Polysciences, Inc. Warrington, PA, USA). All slides were imaged using a Panoramic 250 High Throughput Scanner (3DHitech Ltd, Budapest, Hungary) and images were taken at x20 magnification using Panoramic Viewer software (Version 1.15.4, Budapest, Hungary) for analysis using Image J software (NIH, USA).

Conjugated wheat germ agglutinin (WGA; wheat germ agglutinin, CF488A; Biotium, Cambridge, UK) staining was applied to outline muscle boundaries and isolectin B4 (IB4, Vector B-1205, Vector Laboratories Ltd., Peterborough, UK) for capillaries. All slides were imaged using the confocal microscope LSM510 (Carl Zeiss, Germany) and images were captured at x20 magnification for analysis using Image J software (NIH, USA). Number of capillaries per muscle fibre was manually counted in a blinded fashion.

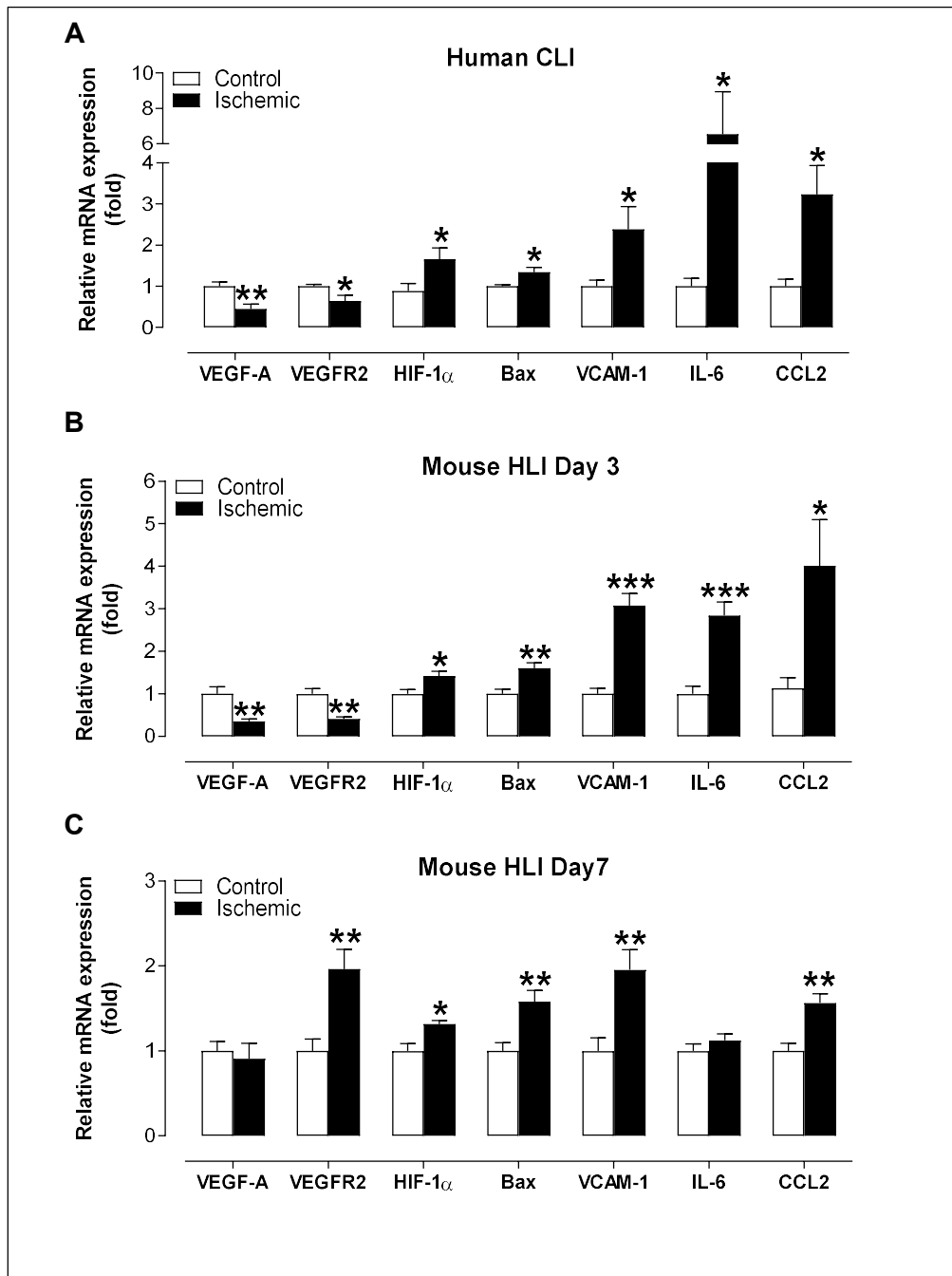
Immunofluorescence was used to localize NPR-C (anti-NPR-C, ab37617, 1:100; Abcam), in the blood vessels using anti-CD31 (platelet endothelial cell adhesion molecule, PECAM-1, ab9498, Abcam, 1:20) and in the gastrocnemius

muscle using WGA (RL-1022, Vectorlabs, 1:50). Following routine removal of paraffin and antigen retrieval using citrate-based solution (pH6.0, Vectorlabs, UK), human gastrocnemius muscle sections were permeabilized for 10 min in 0.2% Triton X-100, in blocking solution (10% goat serum/1% bovine serum albumin (BSA) in PBS) at room temperature for 1 h and probed with the primary antibodies diluted in the blocking solution overnight at 4°C. After primary antibody incubation, sections were washed with PBS for three times and incubated with appropriate Alexa Fluor-coupled secondary antibodies (1:400, Molecular Probes) for 1 h at room temperature. To counteract auto-fluorescence, sections were incubated in 0.3% Sudan black. Nuclei were counterstained with DAPI. Sections were thoroughly washed with PBS before mounting them with ProLong mounting media (ThermoFisher Scientific, UK).

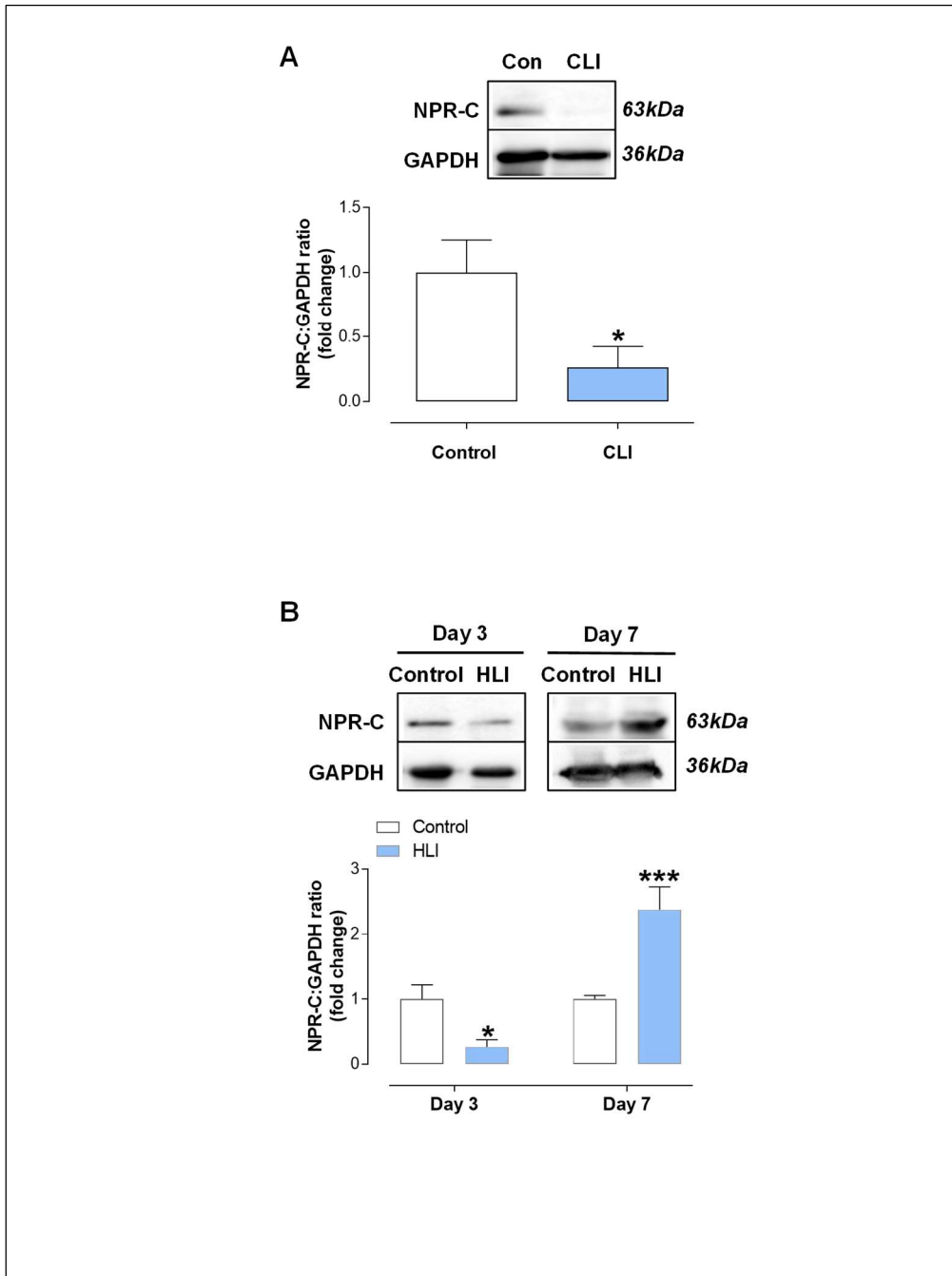
SUPPLEMENTAL FIGURES



Supplemental Figure 1. Knockdown of natriuretic peptide receptor (NPR)-B and NPR-C in human umbilical vein endothelial cells. Relative expression of natriuretic peptide receptor (NPR)-C (**A**) mRNA and (**B**) protein, and NPR-B mRNA (**C**) in human umbilical vein endothelial cells (HUVEC) following siRNA knockdown (KD) in comparison to administration of a nonsensical RNA sequence (NS) demonstrating effective gene deletion. (**D**) C-type natriuretic peptide (CNP; 1 nM) promotes tubule formation in HUVECs in the absence and presence of NPR-B KD. Data are presented as mean \pm SEM. Statistical analyses by Student's t-test (**A-C**) and one-way ANOVA with Bonferroni post hoc test (**D**) with * $P < 0.05$, ** $P < 0.01$, *** $P < 0.001$ versus NS siRNA (n=5).

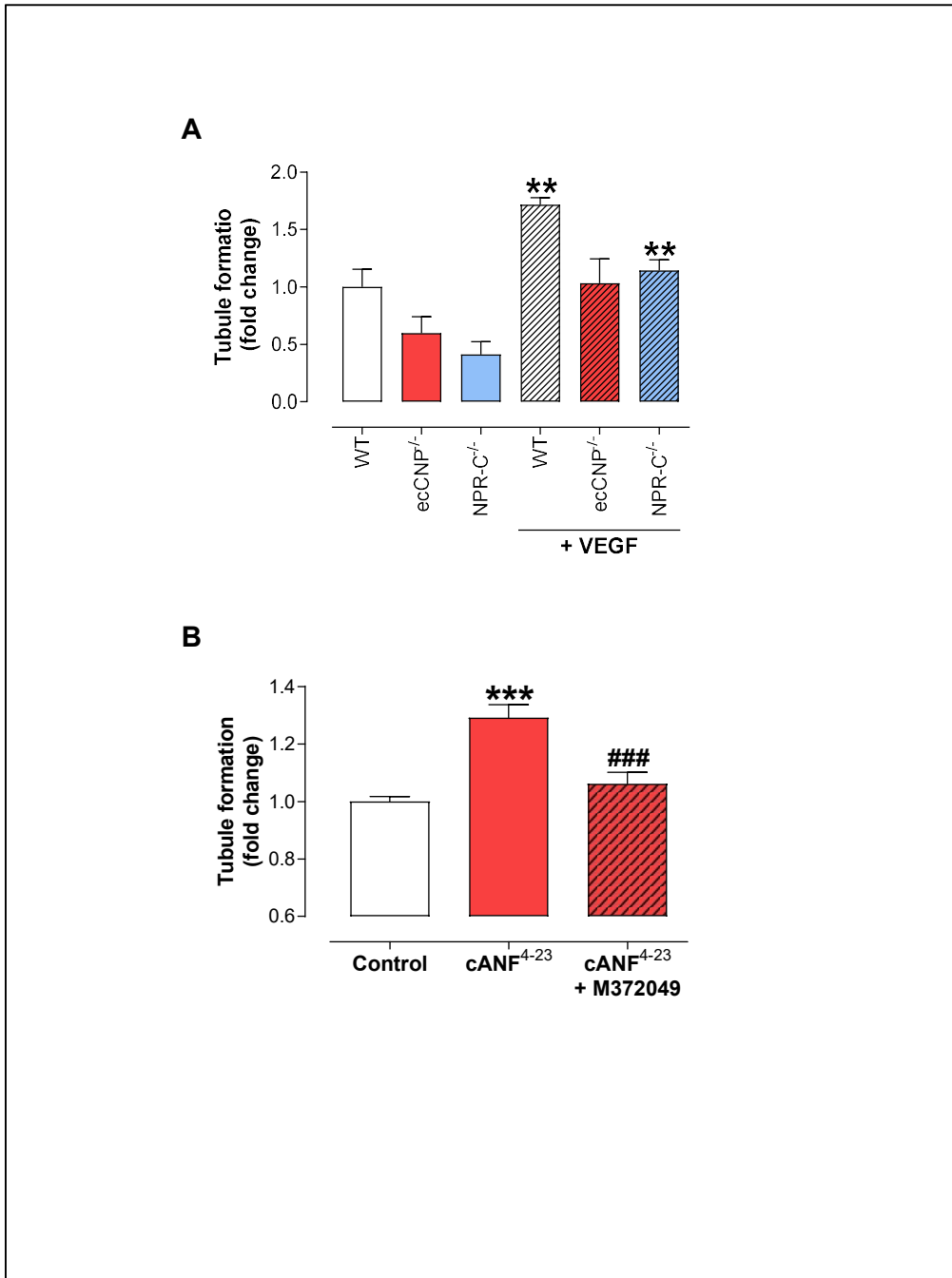


Supplemental Figure. 2. Changes in angiogenic gene expression in human critical limb ischemia patients and murine hindlimb ischemia. Relative expression of vascular endothelial growth factor (VEGF)-A, VEGF receptor (VEGFR)2, hypoxia inducible factor (HIF)-1 α , Bax, vascular cell adhesion molecule (VCAM)-1, interleukin (IL)-6 and chemokine (C-C motif) ligand (CCL)2 mRNA in the (A) gastrocnemius muscle of critical limb ischemia (CLI) patients and healthy controls (n=6-7), gastrocnemius muscle of wild type (WT) mice at (B) day 3 and (C) day 7 following hindlimb ischemia (HLI) (n=6-7). Data are presented as mean \pm SEM. Statistical analyses by Student's t-test with *P<0.05, **P<0.01, ***P<0.001 versus corresponding control.

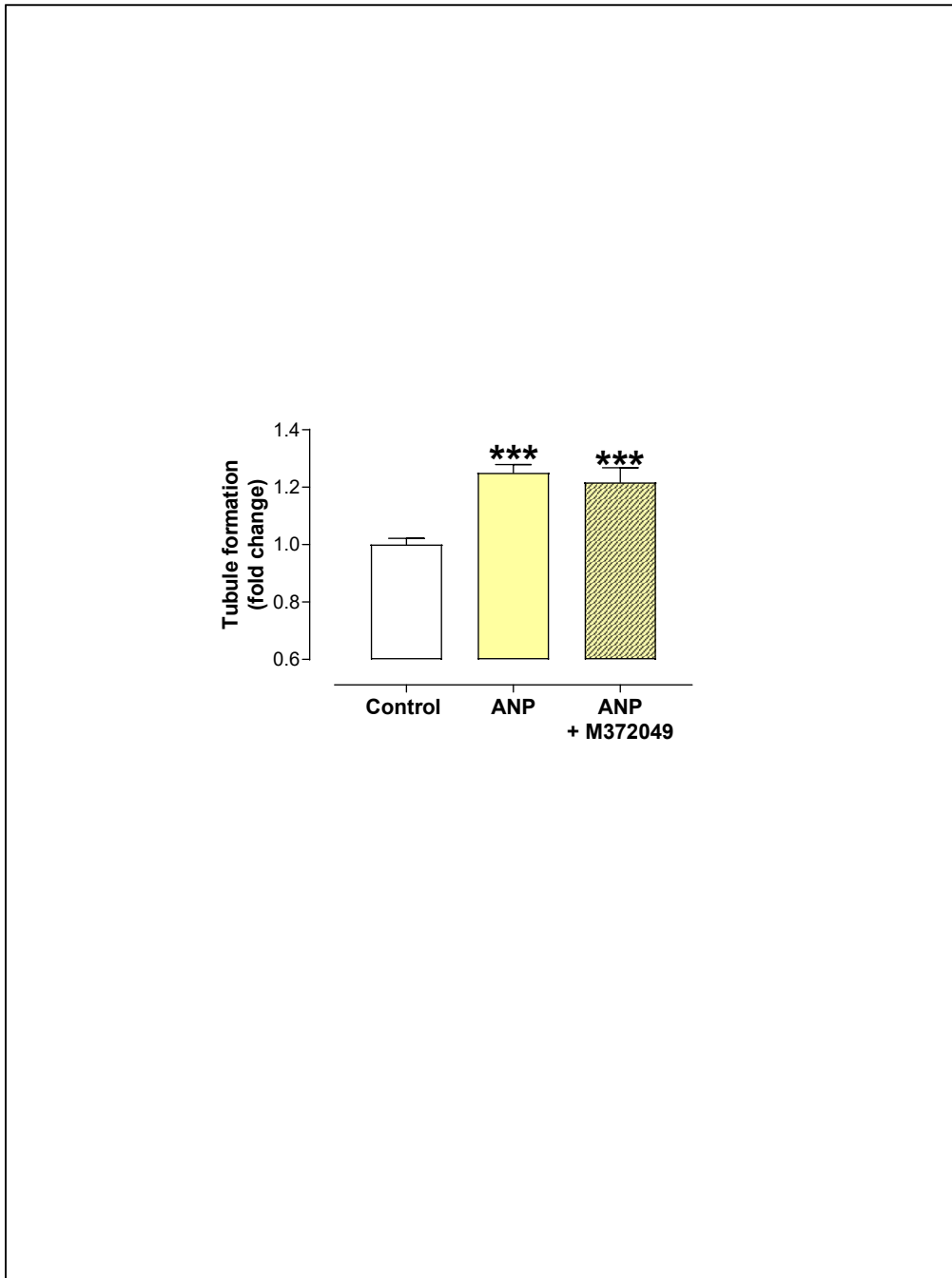


Supplemental Figure 3. Changes in natriuretic peptide receptor-C expression in human critical limb ischemia patients and murine hindlimb ischemia (A)

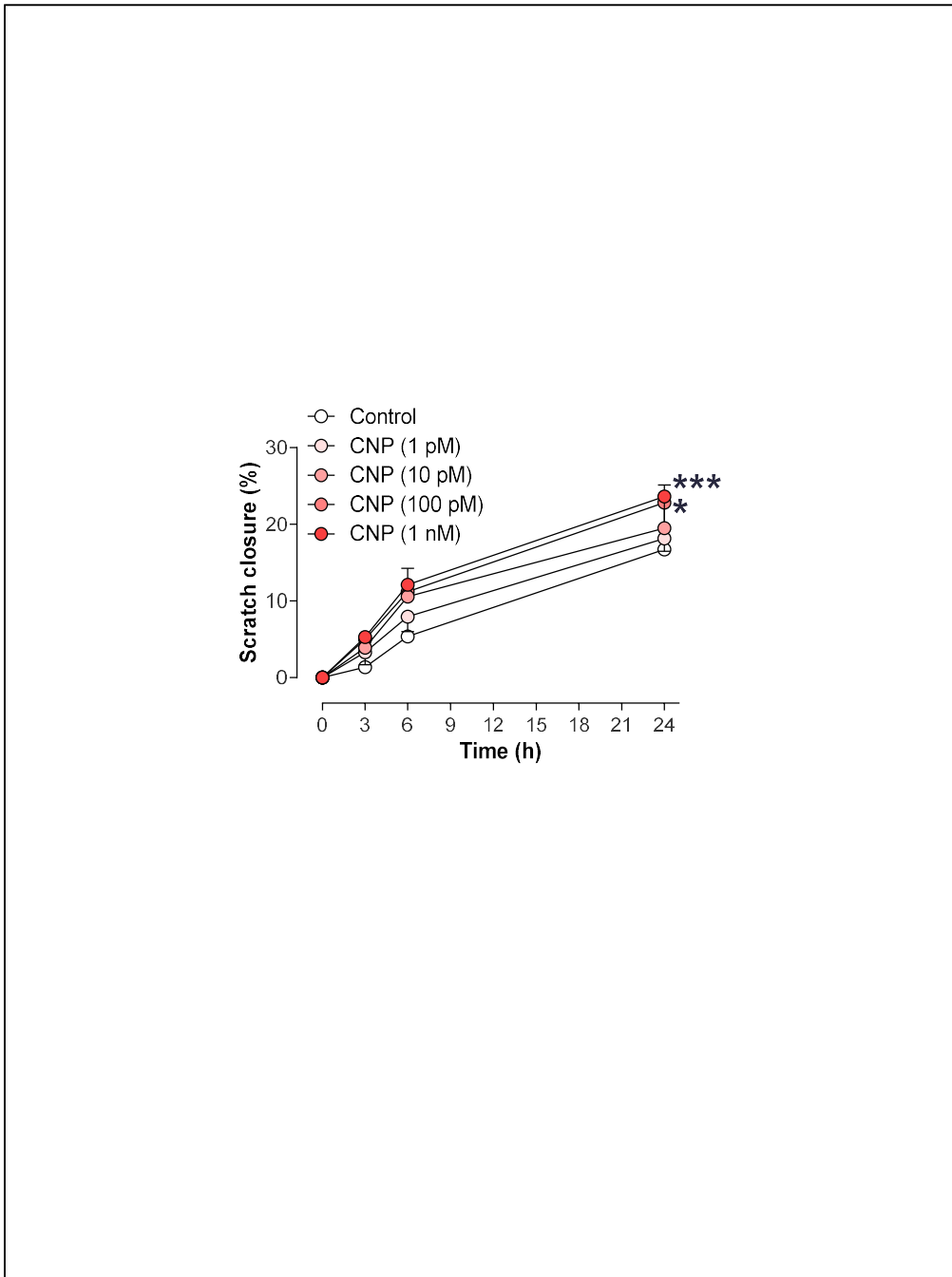
Natriuretic peptide receptor (NPR)-C protein expression is markedly reduced in gastrocnemius muscle biopsies of critical limb ischemia (CLI) patients compared to healthy subjects (Control; n=6-7), and **(B)** NPR-C protein is reduced in ischemic gastrocnemius muscles (HLI) from wild type (WT) mice at day 3, compared to non-ischemic controls (Control), with a significant increase at day 7 following HLI (n=5-7). Data are presented as mean \pm SEM. Statistical analyses by **(A)** Student's t-test and **(B)** one-way ANOVA with Bonferroni post hoc test with *P<0.05, ***P<0.001 versus control or WT.



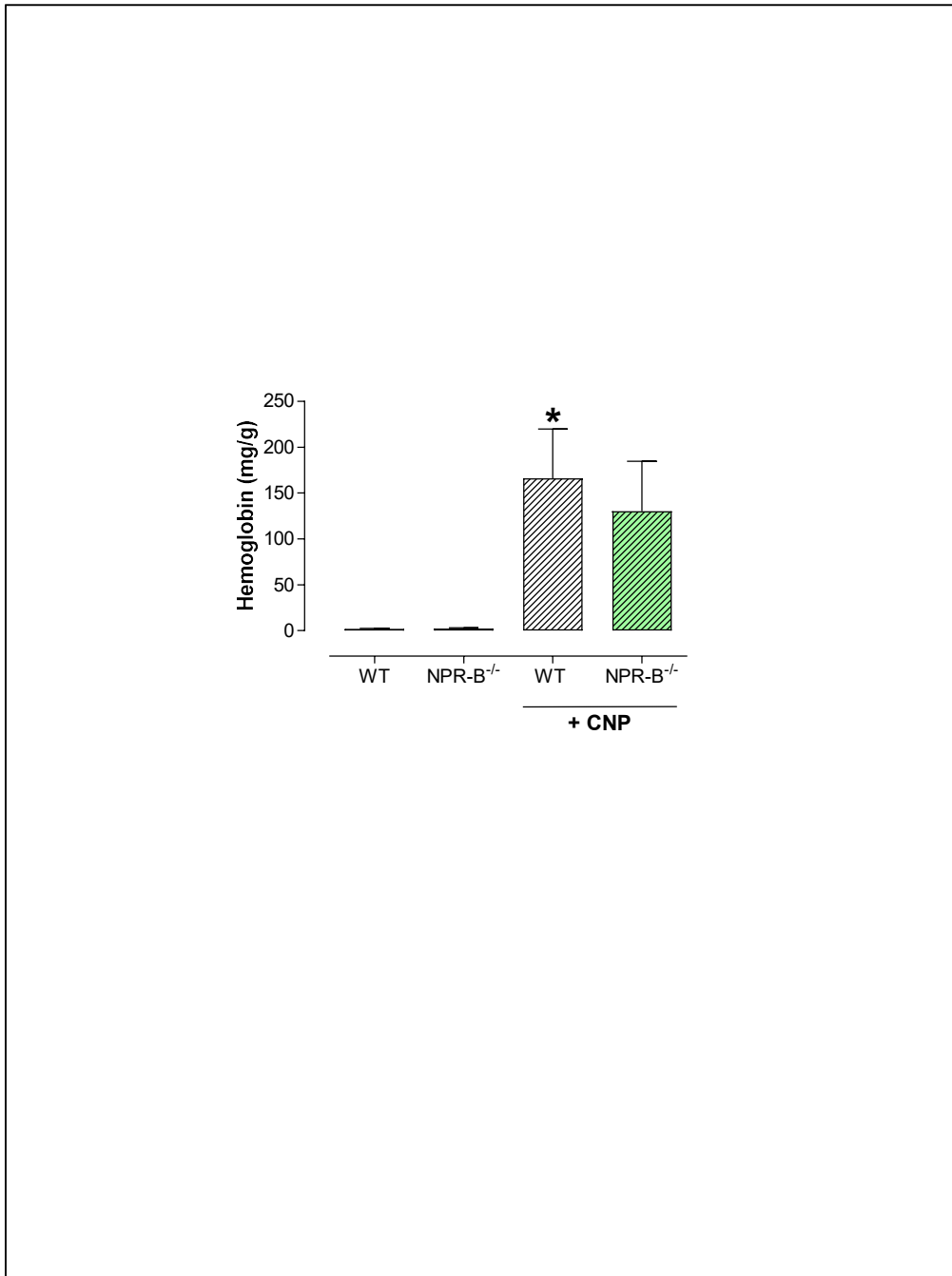
Supplemental Figure 4. Tubule formation in human umbilical vein endothelial cells is impaired by genetic or pharmacological blockade of C-type natriuretic peptide/natriuretic peptide receptor-C signalling. Tubule formation in human umbilical vein endothelial cells (HUVEC) is **(A)** promoted by vascular endothelial growth factor (VEGF; 30 ng/mL) in the presence and absence of endothelium-derived C-type natriuretic peptide (CNP) or natriuretic peptide receptor (NPR)-C, and **(B)** stimulated by the selective NPR-C agonist cANF⁴⁻²³ (1 nM) and blocked by the selective NPR-C antagonist M372049 (10 μ M). Data are presented as mean \pm SEM. Statistical analyses by one way ANOVA with Bonferroni post hoc test with **P<0.01, ***P<0.001 versus corresponding control or genotype and ###P<0.001 versus cANF⁴⁻²³ alone (n=6).



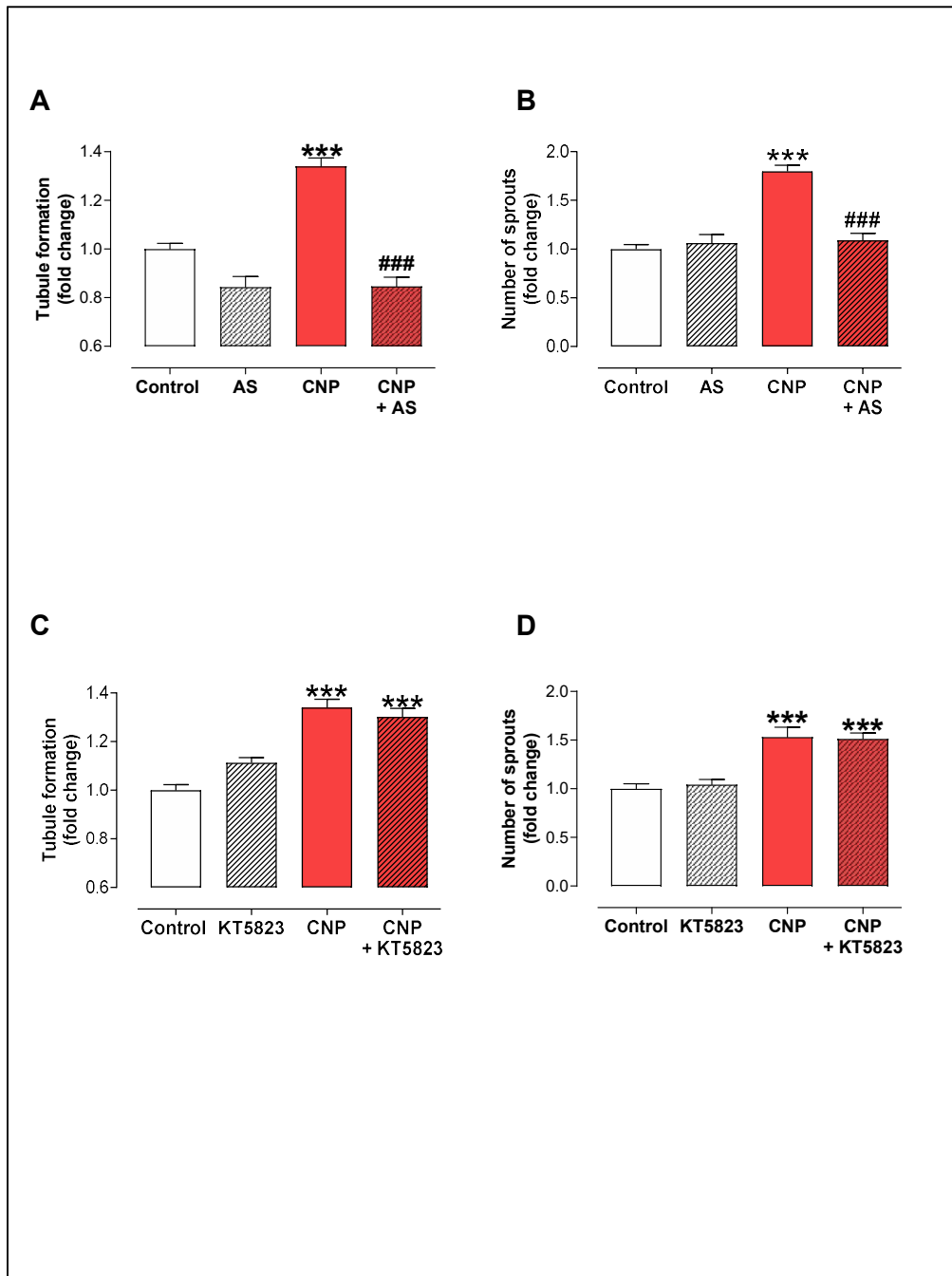
Supplemental Figure 5. Atrial natriuretic peptide does not trigger natriuretic peptide receptor-C-dependent angiogenic responses. Tubule formation in human umbilical vein endothelial cells (HUVEC) is promoted by atrial natriuretic peptide (ANP; 10 nM) but this is not blocked by the selective natriuretic peptide receptor (NPR)-C antagonist M372049 (10 μ M). Data are presented as mean \pm SEM. Statistical analyses by one way ANOVA with Bonferroni post hoc test with *** $P < 0.001$ versus control (n=6).



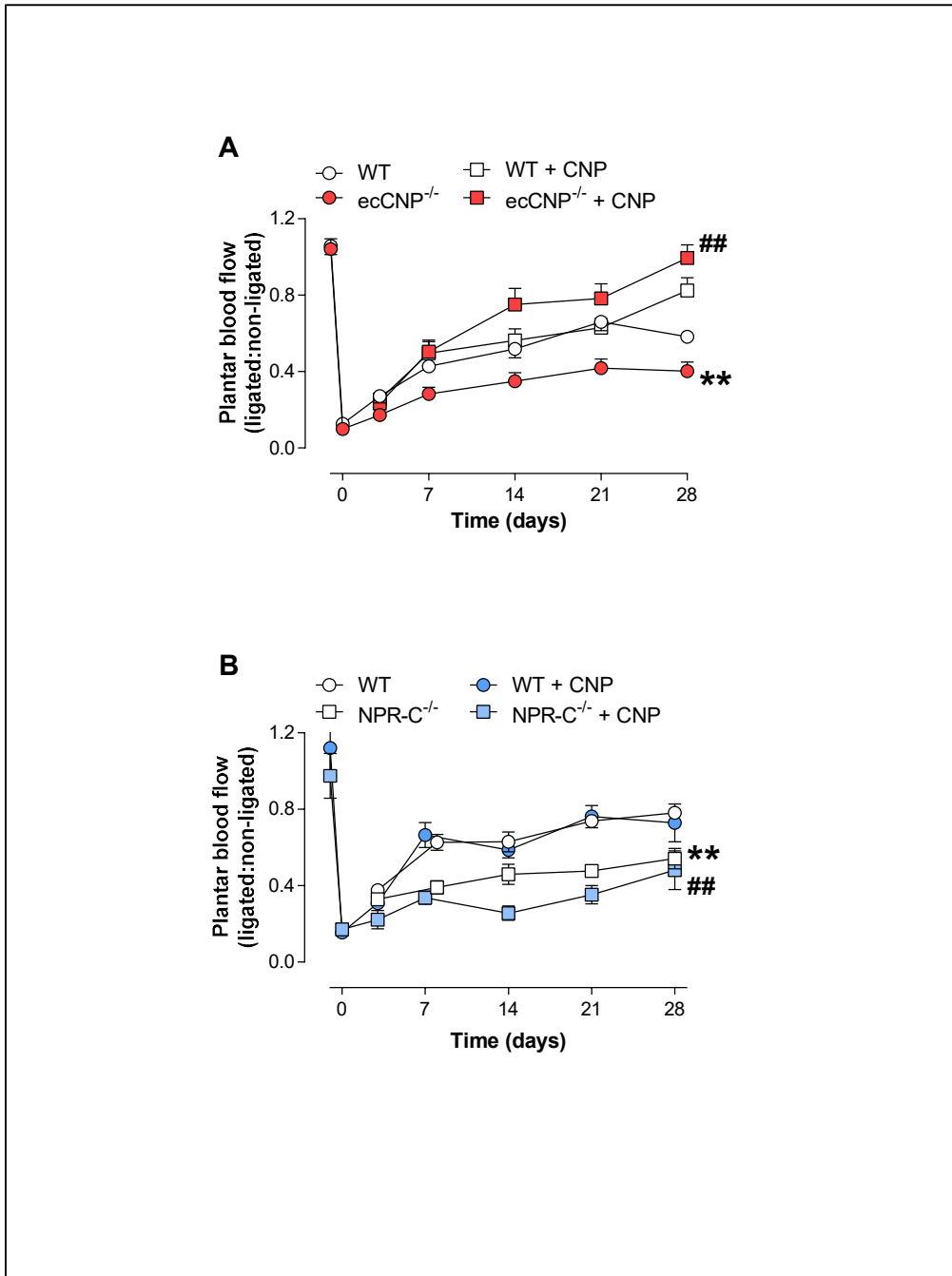
Supplemental Figure 6. C-type natriuretic peptide facilitates endothelial cell migration in a concentration-dependent manner. C-type natriuretic peptide (CNP; 1 pM-1 nM) increases wild type (WT) murine pulmonary microvascular endothelial cell (PMEC) migration (i.e. scratch closure). Statistical analyses by two-way ANOVA with * $P < 0.05$, *** $P < 0.001$ versus control (n=6).



Supplemental Figure 7. C-type natriuretic peptide promotes angiogenesis *in vivo*. C-type natriuretic peptide (CNP; 1 nM) facilitates neovascularisation of matrigel plugs *in vivo* in wild type (WT) and global natriuretic peptide receptor-B knockout (NPR-B^{-/-}) mice as interrogated by hemoglobin content. Data are presented as mean \pm SEM. Statistical analyses by one way ANOVA with Bonferroni post hoc test with *P<0.05 versus corresponding genotype in the absence of CNP (n=3-6).

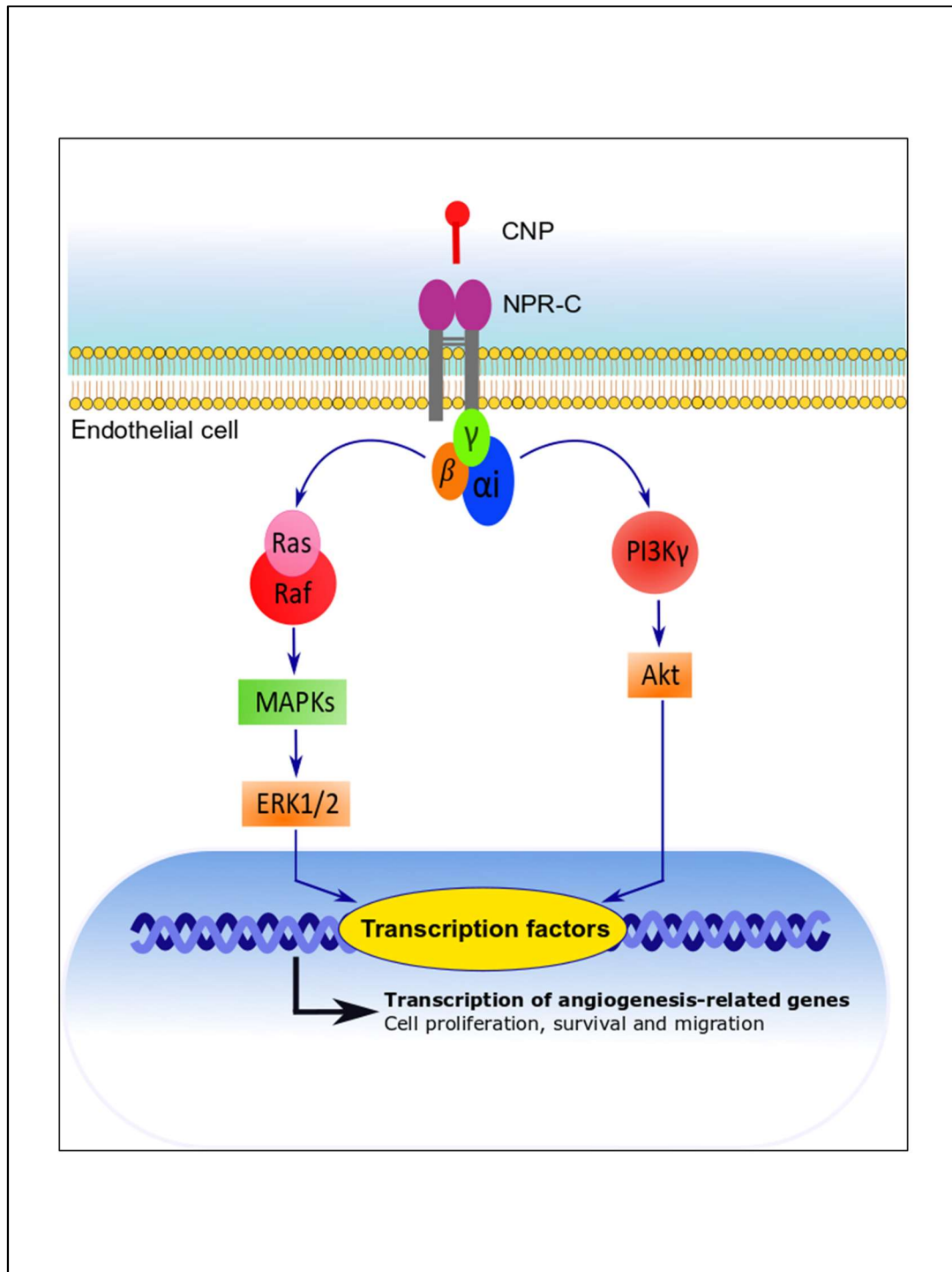


Supplemental Figure 8. *In vitro* angiogenic responses to C-type natriuretic peptide are dependent on phosphoinositide 3-kinase γ but not cGMP-dependent protein kinase. Tubule formation in human umbilical vein endothelial cells (HUVEC) and aortic sprouting is **(A & B)** sensitive to the selective phosphoinositide 3-kinase (PI3K) γ inhibitor AS605240 (AS; 100nM) but **(C & D)** insensitive to the selective cGMP-dependent protein kinase (PKG) inhibitor KT5823 (2 μ M). Statistical analyses by one way ANOVA with Bonferroni post hoc test with ***P<0.001 versus control and ###P<0.001 versus CNP alone (n=6).



Supplemental Figure 9. C-type natriuretic peptide (CNP) reverses the impaired recovery of blood flow following hindlimb ischemia in endothelium-specific CNP knockout, but not global natriuretic peptide receptor-C knockout, mice.

Restoration of plantar blood flow is impaired in **(A)** endothelium-specific C-type natriuretic peptide knockout (ecCNP^{-/-}) mice and **(B)** global natriuretic peptide receptor-C knockout (NPR-C^{-/-}) animals compared to wild type (WT) littermates but this deficit can only be phenotypically-rescued by administration of CNP (0.2mg/kg/day) in ecCNP^{-/-} mice. Data are presented as mean ± SEM. Statistical analyses by two-way ANOVA with **P<0.01 versus WT and ##P<0.01 versus WT + CNP (n=6-12).



Supplemental Figure 10. Schematic representation of the novel CNP/NPR-C/G_i-triggered pro-angiogenic signaling pathways identified and characterized herein. C-type natriuretic peptide, CNP; natriuretic peptide receptor-C, NPR-C; G-protein subunits, $\alpha\beta\gamma$; mitogen-activated protein kinase, MAPK; extracellular signal-regulated kinase 1/2, ERK1/2; phosphoinositide 3-kinase γ , PI3K γ .

SUPPLEMENTAL TABLE

Target gene	Primer sequence (5'-3')	Accession number
Human Bax	Forward: CGGGTTGTCCCTTTTCTA Reverse: GGACATCAGTCGCTTCAGTG	NM_001291428.1
Mouse Bax	Forward: TGCAGAGGATGATTGCTGACG Reverse: AGCCACCCTGGTCTTGGAT	NM_007527.3
Human CNP	Forward: TACAAAGGAGCCAACAAGAAGG Reverse: AAAGATGACCTCAGCACAACG	NM_024409.3
Mouse CNP	Forward: AAAAGGGTGACAAGACTCCAGGCAG Reverse: GGTGTTGTGTATTGCCAGTA	NM_010933.5
Human CCL2	Forward: CTCAGCCAGATGCAATCAATG Reverse: TGAACCCACTTCTGCTTGGG	NM_002982.3
Mouse CCL2	Forward: GAAGCTGTAGTTTTTGTCCCA Reverse: TTCCTTCTTGGGGTCAGCAC	NM_011333.3
Human HIF-1α	Forward: ATCACCTCTTCGTCGCTTC Reverse: TCCAATCACCCAGCATCCAGAA	NM_181054.2
Mouse HIF-1α	Forward: TCTGGATGCCGGTGGTCTA Reverse: AAAAAGCTCCGCTGTGTGTT	NM_001313920.1
Human IL-6	Forward: GGTACATCCTCGACGGCATC Reverse: CACCAGGCAAGTCTCCTCAT	NM_000600.4
Mouse IL-6	Forward: TCGTGGAAATGAGAAAAGAGTTGTG Reverse: ACTCCAGAAGACCAGAGGAAA	NM_001314054.1
Human NPR-B	Forward: ACGGGCGCATTGTGTATATC Reverse: GGGCTCTTATCAGCAGACGA	NM_003995.3
Mouse NPR-B	Forward: CCCTGTGCCTTTGACTTGGGA Reverse: GCAACAACATTTCCAGCGA	NM_001355466.1
Human NPR-C	Forward: TTGCACACGTCCATCTACAGT Reverse: CTCTTCCATGAGCCATCTCCATA	NM_001204375.1
Mouse NPR-C	Forward: GGGGGTCCACGAGGTTTTTC	NM_008728.2

	Reverse: CTCCACGAGCCATCTCCGTA	
Human VCAM-1	Forward: GGATAATGTTTGCAGCTTCTCAAG Reverse: TTCGTACCTTCCCATTCAAGT	NM_001078.3
Mouse VCAM-1	Forward: TGGTCAAATGGAATCTGAACC Reverse: CCCAGATGGTGGTTTCCTT	NM_011693.3
Human VEGF-A	Forward: TGTGAATGCAGACCAAAGAAAG Reverse: ACCAACGTACACGCTCCAG	NM_001025366.2
Mouse VEGF-A	Forward: GCAGATGTGAATGCAGACCAA Reverse: TTCTCCGCTCTGAACAAGGC	NM_001110267.1
Human VEGFR2	Forward: TCTGCCTACCTCACCTGTTTC Reverse: TGTCCGTCTGGTTGTCATCTG	NM_002253.3
Mouse VEGFR2	Forward: CATACCGCCTCTGTGACTTCT Reverse: GCTGTCCCCTGCAAGTAATCT	NM_010612.2
Human & mouse RPL19	Forward: GGTTGCCTCTAGTGTCTCC Reverse: TTGGCGATTTTCATTGGTCTCA	NM_000981.4 & NM_001159483.1

Supplemental Table 1. Primer sequences used for qRT-PCR analyses. C-type natriuretic peptide, CNP; chemokine (C-C motif) ligand 2, CCL2; hypoxia inducible factor-1 α , HIF-1 α ; interleukin-6, IL-6; natriuretic peptide receptor-B, NPR-B; natriuretic peptide receptor-C, NPR-C; vascular cell adhesion molecule-1, VCAM-1; vascular endothelial growth factor-A, VEGF-A; VEGF receptor 2, VEGFR2; ribosomal protein L19, RPL19.

SUPPLEMENTAL REFERENCES

1. Moyes AJ, Khambata RS, Villar I, Bubb KJ, Baliga RS, Lumsden NG, Xiao F, Gane PJ, Rebstock AS, Worthington RJ, Simone MI, Mota F, Rivilla F, Vallejo S, Peiro C, Sanchez Ferrer CF, Djordjevic S, Caulfield MJ, MacAllister RJ, Selwood DL, Ahluwalia A and Hobbs AJ. Endothelial C-type natriuretic peptide maintains vascular homeostasis. *J Clin Invest.* 2014;124:4039-4051.
2. Geister KA, Brinkmeier ML, Hsieh M, Faust SM, Karolyi IJ, Perosky JE, Kozloff KM, Conti M and Camper SA. A novel loss-of-function mutation in Npr2 clarifies primary role in female reproduction and reveals a potential therapy for acromesomelic dysplasia, Maroteaux type. *Hum Mol Genet.* 2013;22:345-57.
3. Matsukawa N, Grzesik WJ, Takahashi N, Pandey KN, Pang S, Yamauchi M and Smithies O. The natriuretic peptide clearance receptor locally modulates the physiological effects of the natriuretic peptide system. *Proc Natl Acad Sci U S A.* 1999;96:7403-7408.